Vol. 567: 57–78, 2017
https://doi.org/10.3354/meps12054

MARINE ECOLOGY PROGRESS SERIES
Mar Ecol Prog Ser

Published March 13

A novel quantile method reveals spatiotemporal shifts in phytoplankton biomass descriptors between bloom and non-bloom conditions in a subtropical estuary

Natalie G. Nelson[1], Rafael Muñoz-Carpena[1,*], Edward J. Phlips[2]

[1]Hydrology & Water Quality, Agricultural & Biological Engineering, University of Florida, Gainesville, Florida 32611, USA
[2]Fisheries & Aquatic Sciences, School of Forest Resources & Conservation, University of Florida, Gainesville, Florida 32653, USA

ABSTRACT: Estuarine environments support dynamic phytoplankton blooms, especially in low-latitude regions, where the effects of local drivers dominate. Identifying key bloom drivers from entangled ecological and anthropogenic influences is particularly challenging in stressed systems where several disturbances interact. Additionally, processes controlling bloom and non-bloom phytoplankton biomass dynamics can differ spatially, further confounding characterization of disturbance regimes that create bloom-favorable conditions. This study aims to explore the question of whether the shift from non-bloom to bloom conditions is matched by a shift in the relative importance of water quality drivers. Florida Bay (USA), a shallow subtropical inner shelf lagoon, was chosen as the study site due to its unique bloom dynamics and low-latitude location, as well as for the availability of long-term (16 yr) water quality data consisting of monthly measurements from 28 locations across the 2200 km^2 bay. At each of the locations, we applied a novel threshold-based quantile regression analysis to chlorophyll *a* data to define bloom conditions, separate data from non-bloom conditions, and evaluate phytoplankton biomass dynamics of each of the 2 states. The final suite of explanatory covariates revealed spatial trends and differences in the relative importance of water quality descriptors of phytoplankton between the 2 conditions. The effects of turbidity and salinity on phytoplankton biomass became pronounced during blooms, whereas non-bloom conditions were primarily explained by autoregressive phytoplankton biomass trends and nutrient dynamics. The proposed analytical approach is not limited to any particular aquatic system type, and can be used to produce practical spatiotemporal information to guide management, restoration, and conservation efforts.

KEY WORDS: Quantile regression · Time series modeling · Spatial patterns · Cyanobacteria · Florida Bay

INTRODUCTION

Phytoplankton biomass dynamics in estuarine environments reflect the highly dynamic and complex nature of these ecosystems. Inter- and intra-annual trends in estuarine phytoplankton biomass typically respond more strongly to local influences than to regional forcing (Cloern & Jassby 2008), particularly in low-latitude regions, where seasonal climatic variability is not strong enough to override other local influences (Cloern & Jassby 2010). Contributing local effects include nutrient delivery from oceanic upwelling and terrestrial freshwater flows (Cloern 1996), connectivity to developed coastal basins, and, in shallow systems, wind-induced mixing and benthic-pelagic coupling (Cloern 1982, Thompson et al.

*Corresponding author: carpena@ufl.edu

2008). In contrast, phytoplankton biomass in high-latitude lakes and the open ocean is often dictated by climatic periodicity (Cloern & Jassby 2008, Winder & Cloern 2010).

The balance between local effects and regional forcing is captured in chlorophyll *a* (chl *a*) data. While annual variability in chl *a* reflects the level of disturbance of a system (high inter-annual chl *a* variability corresponds to high disturbance), seasonal chl *a* variability reflects the annual climate cycle in a system (low seasonal variability corresponds to weak intra-annual climatic variability). Cloern & Jassby (2010) evaluated temporal patterns of phytoplankton biomass in 51 estuarine and nearshore ecosystems by comparing annual and seasonal chl *a* variability and found that, of all the considered systems, Florida Bay had the highest annual to seasonal chl *a* variability ratio. This characterization indicates that Florida Bay is a disturbed system lacking a pronounced intra-annual climatic signal. Though this diagnosis was formulated solely from evaluating the inter- and intra-annual variability of monitoring data, reviews of Florida Bay's ecological health point to a similar conclusion (Boesch et al. 1993, Rudnick et al. 2005, Glibert et al. 2009). Florida Bay has suffered from sporadic instances of acute ecological disturbance in the form of phytoplankton blooms and other modes of degradation (Butler et al. 1995, Fourqurean & Robblee 1999, Hall et al. 1999, Glibert et al. 2009), and its low-latitude location in the subtropics corresponds to relatively weak seasonal climatic forcing. The combination of (1) phytoplankton growth that remains minimally controlled by climatic variability and (2) the periodic presence of ecologically disruptive phytoplankton blooms makes Florida Bay an exceptionally dynamic environment and ideal study site for investigations on estuarine phytoplankton biomass dynamics.

Concern over Florida Bay's ecological resiliency to mounting anthropogenic influences has motivated field studies, statistical analyses, and mechanistic modeling of diverse aspects of phytoplankton ecology in the bay. Field observations show that, since the 1980s, recurrent blooms of unicellular picoplanktonic cyanobacteria (e.g. *Synechococcus* spp.; Phlips et al. 1999) have driven a variety of disruptive ripple effects, such as reductions in seagrass communities, widespread sponge mortality, and related losses of juvenile spiny lobster habitat (Butler et al. 1995). Model analyses have furthered these findings by considering the interplay between changing seagrass and phytoplankton distributions (Madden & McDonald 2009), bloom dynamics along the northern shore (Melesse et al. 2008), and the influence of climatic patterns on phytoplankton biomass (Briceño & Boyer 2010). Additional statistical investigations of the relationships between phytoplankton and water quality have primarily involved principal component (Boyer et al. 1997, 1999) or empirical orthogonal function analyses (Burd & Jackson 2002).

These prior studies have enhanced the qualitative understanding of phytoplankton ecology in Florida Bay and beyond, but there exists a gap in the quantification of the changes in relative importance of drivers between bloom and non-bloom states. Outstanding questions include: (1) are important water quality drivers of blooms equally important under non-bloom conditions; and (2) does the extent to which water quality drivers vary in importance between bloom and non-bloom conditions change spatially? These questions broadly apply to other estuarine systems due to the aforementioned challenges associated with analyzing water quality data from low-latitude environments characterized by irregular phytoplankton biomass trends (Cloern & Jassby 2010).

The goal of the present study was to comparatively investigate bloom and non-bloom states to infer changes between these 2 conditions introduced by water quality drivers. The specific objectives were to: (1) objectively identify a threshold that separates bloom from non-bloom conditions, (2) reveal spatio-temporal differences in phytoplankton–environmental relationships between non-bloom and bloom conditions, using Florida Bay as a case study, and (3) quantitatively identify linkages between water quality descriptors of blooms in subtropical lagoon systems. To address these objectives, we developed and applied a novel modification of quantile regression (Koenker & Bassett 1978, Cade & Noon 2003) to understand spatial and temporal long-term phytoplankton biomass trends across Florida Bay. Quantile regression has recently been applied to identify limiting factors of phytoplankton blooms in European lakes (Carvalho et al. 2013) and Lake Champlain, USA (Xu et al. 2015). These applications analyzed narrow quantiles across the distribution of observed chl *a* in their respective systems. In contrast, the modification proposed herein identifies a bloom-relevant quantile threshold to separate chl *a* observations into bloom and non-bloom classes. Furthermore, this modification allows for the study of spatiotemporal differences in drivers underlying bloom versus non-bloom conditions. This analytical framework expands the applicability of quantile regression for coastal water quality management purposes, and can

be widely applied to other systems afflicted by algal blooms. In particular, researchers and environmental data scientists will find this framework useful for objectively and quantitatively evaluating seemingly chaotic phytoplankton biomass data lacking a temperature-driven annual signal, which are typical of low-latitude estuaries.

MATERIALS AND METHODS

Site description

Florida Bay is a 2200 km^2 (Rudnick et al. 1999) inner shelf lagoon located at the intersection of the Everglades, Florida Keys, Gulf of Mexico, and Atlantic Ocean at the tip of the Florida peninsula (Fig. 1A). A mixture of mud banks, seagrass beds, and hard-bottom and soft-bottom habitat compose the benthos. The network of mud banks and mangrove islands throughout the bay (Fig. 1B) delineates approximately 44 basins that have distinct water circulation patterns (Nuttle et al. 2000). Circulation patterns in some of the individual basins are partially defined by differences in freshwater inputs from canals, creeks, and sloughs flowing from the Everglades and South Florida (Nuttle et al. 2000, Kelble et al. 2007). The bay receives much of its terrestrial freshwater inflow from Taylor Slough and the C-111 Canal (Rudnick et al. 1999), and saline fluxes from the Gulf of Mexico and Atlantic Ocean (Lee et al. 2006). However, human development and water management practices in Central and South Florida have starved the Everglades of freshwater over the past century, and, as a result, reduced Florida Bay's freshwater inputs to only a fraction of the historical flow (McIvor et al. 1994).

Reductions in historical freshwater inputs to the bay have resulted in increased salinity, particularly in basins with limited tidal interactions with the surrounding coastal marine environment. The impact of reduced freshwater influence is further exacerbated by the shallow nature of the estuary (Nuttle et al. 2000), with the average depth across the bay being approximately 1.4 m (Hansen & DeWitt 2000). Being downstream from the Everglades, Florida Bay is impacted by Comprehensive Everglades Restoration Plan (CERP 2005) activities (FBFKFS 2002), which include projects aimed at re-introducing historical freshwater flows to the Everglades and Florida Bay as well as reducing bloom occurrence.

Analyses of spatial patterns of key environmental factors in Florida Bay have divided the bay into regions of observed similarity through different characteristics, such as phytoplankton communities (Phlips et al. 1995), seagrass distributions (Zieman et al. 1989), and water quality trends (Boyer et al. 1997). Regions based on those described by Phlips et al. (1995) were employed for this study to segregate the bay into 5 regions, i.e. northeast, east, north central, south central, and west (Fig. 1A). The West Bay experiences nitrogen limitation, whereas the East Bay is phosphorus-limited (Lavrentyev et al. 1998, Boyer et al. 1999). The East Bay is starved of phosphorus primarily as a function of its calcium-carbonate-rich sediments (Zhang et al. 2004), which bind phosphorus and render it unavailable for organic assimilation. The nutrient limitation gradients converge in the Central Bay and cause seasonal fluctuation between nitrogen and phosphorus limitation (Boyer et al. 1999). Shifts in phytoplankton community composition occur along the bay's nutrient limitation gradients. Phlips & Badylak (1996) surveyed phytoplankton communities across Florida Bay and determined that the western edge of the bay was dominated by diatoms, the Central Bay by cyanobacteria (primarily *Synechoccocus* spp., a unicellular picoplanktonic cyanobacterium), and the eastern region by a mixed community of diatoms, dinoflagellates, and picocyanobacteria. An exceptionally severe bloom in the East Bay that persisted from 2005 to 2008 was found, like the central region of the bay, to be dominated by *Synechococcus* spp. (Glibert et al. 2009).

Spatial variability in environmental factors explains some of the observed trends in phytoplankton community structure. The West Bay is highly flushed, moderately turbulent, and has relatively stable marine-like salinities due to its location alongside the Gulf of Mexico (Phlips & Badylak 1996). These characteristics create an ideal environment for the diatoms of Florida Bay, which have narrow salinity tolerances, strong light use efficiency, and require wave energy to avoid sedimentation due to their lack of motility and heavy siliceous cell structures (Phlips & Badylak 1996, Richardson 2009). In contrast, many interacting factors are believed to underpin the prevalence of cyanobacteria in the central region of the bay. Euryhaline character and buoyancy control (Phlips & Badylak 1996, Phlips et al. 1999), high nutrient uptake affinities (Richardson 2009), and grazer avoidance (Goleski et al. 2010) enable cyanobacteria, particularly *Synechococcus* spp., to thrive in the North Central Bay, a region characterized by long residence times (Lee et al. 2006), periodically heightened salinities (Nuttle et al. 2000, Lee et al. 2006, Kelble et al. 2007), deep deposits of organic material

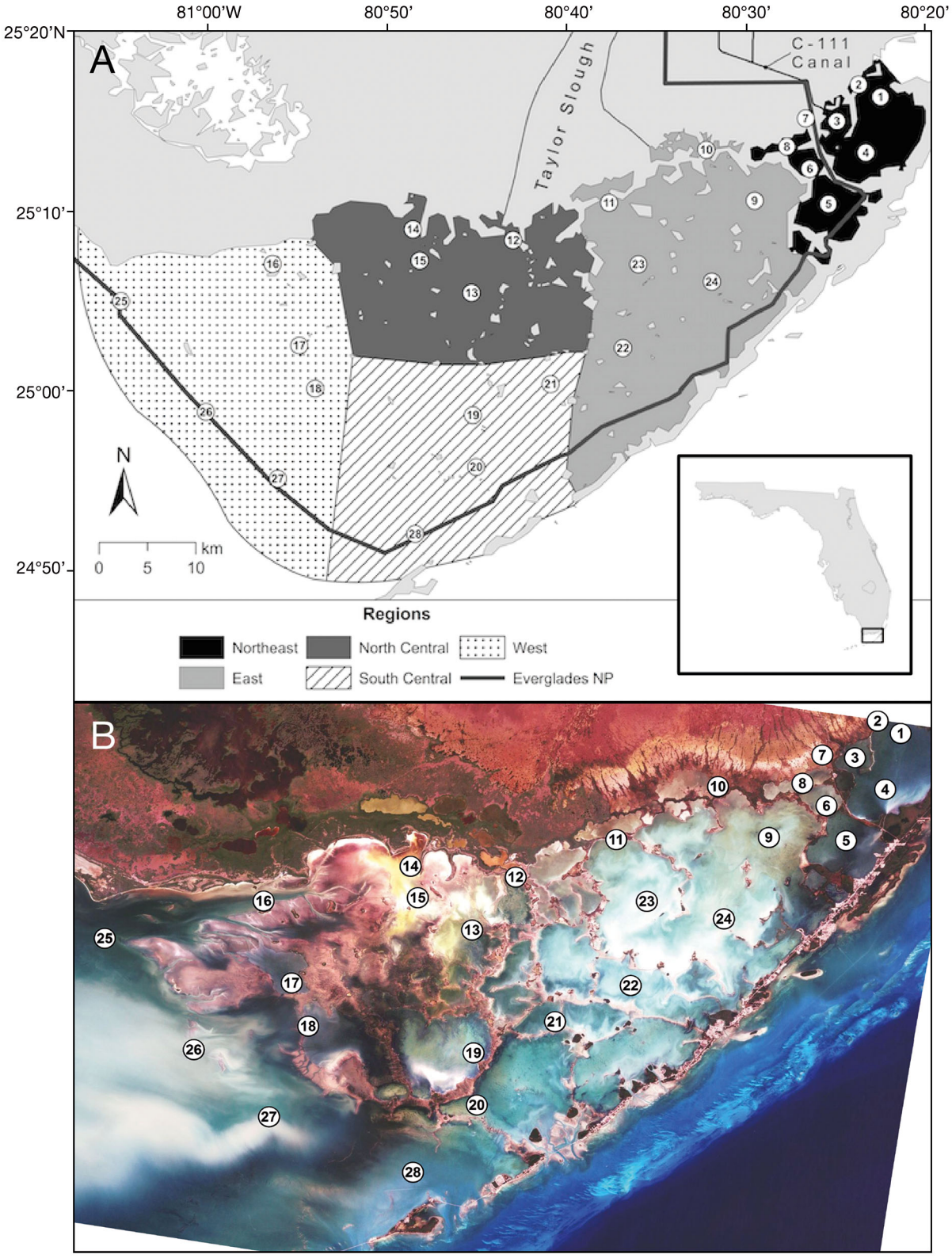

Fig. 1. Map of Florida Bay, Florida (USA). (A) Five regions of similar phytoplankton community structure shown, along with dominant sources of terrestrial freshwater to the Bay (Taylor Slough and C-111 Canal) and the Everglades National Park (Everglades NP) boundary. (B) Satellite imagery of Florida Bay depicting the extensive network of mud banks and mangrove islands (base image: NASA Landsat 7, October 2000). Encircled numbers correspond to the 28 stations

(Phlips & Badylak 1996), and a lack of filter feeders (Peterson et al. 2006). Cyanobacteria in the central region of the bay have also been observed to utilize organic nitrogen and phosphorus (Glibert et al. 2004, Boyer et al. 2006, Goleski et al. 2010). The diversity in the phytoplankton community of the eastern regions of the bay is believed to be driven by severe resource limitation (i.e. extreme phosphorus limitation), which promotes a variety of survival strategies (Lavrentyev et al. 1998).

Dataset description

A water quality monitoring network consisting of 28 spatially distributed stations was maintained in Florida Bay from 1989 to 2008 by the Southeast Environmental Research Center of Florida International University (FIU) (Boyer & Briceño 2007). Included among their monthly measurements were chl *a*, total organic carbon, species of inorganic and organic nitrogen and phosphorus, turbidity, pH, salinity, temperature, and dissolved oxygen. Other variables, such as alkaline phosphatase activity, pH, and silicon dioxide, were measured less frequently and, thus, are excluded from this analysis. An alternative Florida Bay water quality dataset by the NOAA-Atlantic Oceanographic and Meteorological Laboratory (AOML) South Florida Program was also evaluated for this study. Although it includes more recent data (1998 to 2012) than those in the FIU dataset, the AOML data were collected less regularly, making the FIU data more suitable to the analysis described herein.

For this study, monthly water quality data from the FIU Water Quality Monitoring Program (http://serc.fiu.edu/wqmnetwork/SFWMD-CD/index.htm) were used. Data spanning August 1992 through September 2008 (194 time steps per station) were used due to the completeness of the dataset for this time period. Prior to August 1992, some of the 28 stations were not regularly sampled. Specific details on sample handling and analysis are explained in Boyer & Briceño (2007). Missing values (less than 5% of data) were replaced with means between the previous and subsequent time points; in select months wherein multiple observations were made, intra-month values were also replaced with mean values to maintain a monthly time step. Data were locally minimum–maximum normalized prior to conducting the analysis to permit for direct comparison of coefficient values between explanatory variables and stations, using the following equation:

$$x'_k = \frac{x_k - \min(x_k)}{\max(x_k) - \min(x_k)} \quad (1)$$

where x is an array of observed data (e.g. chl *a*), k is the station (ranges from 1 to 28), and x' is the locally normalized data vector.

Modified quantile regression model

Quantile regression is a methodological framework involving the fitting of multiple linear regression models between one set of explanatory variables and different quantiles of the response variable's probability distribution (Koenker & Bassett 1978, Cade & Noon 2003). The primary strength of this method is its ability to identify different rates of change between explanatory and response variables across the response variable's distribution (Cade & Noon 2003). The traditional quantile regression approach evaluates several small quantiles across the response variable's distribution, but these subsets are often too narrow to be relevant in management contexts. The quantile regression modification used in this study evaluates subsets of the response variable distribution that reflect management objectives. The use of this modified method confronted the question of whether phytoplankton biomass in Florida Bay responds to fluctuations in environmental disturbance differently during bloom as compared to non-bloom conditions.

The methodological framework of this management-relevant modification of quantile regression includes the following steps. (1) Inspect the empirical cumulative distribution function of normalized chl *a* (includes locally normalized data collected at all stations) in order to identify a shift in curvilinear behavior, which is assumed to correspond to the point at which phytoplankton biomass conditions transition from non-blooms to blooms. This transition point is designated as the quantile threshold that distinguishes chl *a* observations as 2 separate states: an upper quantile that represents 'bloom' conditions, and a lower quantile that represents 'non-bloom' conditions. (2) Divide each station's chl *a* distribution into bloom and non-bloom quantiles based on the determined threshold. The bay-wide quantile threshold translates into site-specific chl *a* concentrations that vary station by station, which allows for spatial heterogeneities to be taken into account while maintaining perspective of the entire ecosystem. (3) Assess the performance and parsimony of models with different combinations of candidate explanatory variables in order to identify the 'best' set of explana-

tory covariates for the case study. (4) Fit multiple linear regression models consisting of the optimal set of explanatory variables to the upper and lower quantiles of each station's chl *a* distribution, which, in this case, produces 56 models in total. (5) Evaluate each model by quantifying performance and evaluating errors for time dependency. (6) Quantify the relative importance of each explanatory variable under bloom and non-bloom conditions at all stations. Each of these steps is detailed below.

(1) Bay-wide quantile threshold

To divide the chl *a* distributions of the 28 stations into quantiles reflective of blooms and non-blooms, a data-driven threshold at which to segregate the distributions was identified. A previous study by Boyer et al. (2009) also established chl *a* thresholds for Florida Bay using a quartile-based method outlined by the EPA (EPA 2001), whereby the chl *a* value corresponding to the 75th chl *a* percentile of a reference system was designated as the level at which chl *a* values in Florida Bay departed from baseline conditions. We decided not to employ this approach due to the *a priori* percentile threshold it imposes on the data, as well as its need for selection of a reference system. Instead, the locally normalized chl *a* data from all 28 stations were compiled into a single series from which the empirical cumulative distribution function (ECDF) was constructed and objectively evaluated for a breakpoint in curvilinear behavior; this threshold is assumed to be consistent with bloom initiation and continuance. The spatially explicit data were collapsed into a single data series based on the similarity of the right-skew in their probability density functions (Fig. S1 in Supplement 1 at www.int-res.com/articles/suppl/m567p057_supp1.pdf); this method would be inappropriate for evaluating data collected among sites characterized by chl *a* distributions with dramatically differing skews.

A piecewise linear curve was fit to the ECDF to objectively identify a breakpoint that represents the quantile at which the slope of the curve begins to considerably increase. The piecewise curve was refit to 1000 bootstrapped samples of the ECDF to quantify the 95% confidence interval of the breakpoint. The quantile corresponding to the identified break was used as the threshold by which the upper and lower chl *a* quantiles were separated. Although a piecewise linear curve does not track the exact shape of an ECDF or represent the curve in its entirety, this approach effectively screened the distribution for a breakpoint and, thus, was deemed appropriate for the present application. The breakpoint's confidence interval also provided useful information by indicating whether the breakpoint was representative of a distinct change in curvilinear behavior: narrow confidence intervals indicate an acute change in slope, whereas wide intervals point to absent or slow-moving changes.

(2) Station-specific chl *a* concentration thresholds

The bay-wide quantile threshold was applied to the stations' individual chl *a* distributions, and the corresponding chl *a* values were tabulated. The bloom threshold is unique to each station when in units of chl *a*, as opposed to quantile.

(3, 4) Parsimonious model selection

To select the optimal, or 'best,' suite of explanatory variables, all of the regularly sampled water quality covariates included within the dataset were screened with the exception of dissolved oxygen (DO) and total organic carbon (TOC). DO was excluded as it is unclear whether variability in DO in this very shallow ecosystem is a significant driver of phytoplankton biomass. TOC was deemed inappropriate as an explanatory variable since this covariate likely serves as a proxy measurement for chl *a* rather than as an explanatory descriptor of phytoplankton biomass; although other components of TOC (i.e. dissolved organic carbon) may influence phytoplankton biomass dynamics in Florida Bay, the inseparability of chl *a* and TOC, particularly in times of heightened phytoplankton biomass, precluded its inclusion in the model evaluation process. Nitrogen and phosphorus were considered in the form of total nitrogen (TN) and total phosphorus (TP), respectively. This is due to the reported importance of both the organic and inorganic fractions of nitrogen and phosphorus for phytoplankton growth in Florida Bay (Glibert et al. 2004, Boyer et al. 2006), which make these composite values appropriate indicators of the system's nutrient status.

To ensure that the covariates in the reduced dataset were independent and suitable for inclusion in multiple linear regression models, the covariates were evaluated for multicollinearity using the variance inflation factor (VIF) (Montgomery & Peck 1992, Zuur et al. 2007). Candidate explanatory variables with VIF values greater than 5 were excluded

from subsequent analyses (Montgomery & Peck 1992, Zuur et al. 2007). VIF values were calculated for bloom and non-bloom subsets of the data at each of the 28 stations (in total, VIF values were calculated for 56 subsets of the entire Florida Bay dataset).

Every possible explanatory variable combination (ranging from single explanatory variables to the entire explanatory variable dataset) was fed into models of the upper and lower chl *a* quantiles of the 28 stations; thus, 56 models (an upper and lower quantile model for each station) were produced per explanatory variable combination. The simulated data of these 56 models were combined by station to produce 28 simulated chl *a* time series. The coefficient of determination (R^2; Eq. 2) and Bayesian information criterion (BIC; Eq. 3) were calculated for these 28 series, the medians of which were tabulated for every explanatory variable combination:

$$R^2 = 1 - \frac{\sum_{i=1}^{N}(O_i - S_i)^2}{\sum_{i=1}^{N}(O_i - O_{\text{mean}})^2} = 1 - \left(\frac{\text{RMSE}}{\text{SD}}\right)^2 \quad (2)$$

$$\text{BIC} = N \cdot \ln\left(\frac{\sum_{i=1}^{N}(O_i - S_i)^2}{N}\right) + z \cdot \ln(N) \quad (3)$$

where N is the number of observations, O_i is the observed data, O_{mean} is the mean of the observed data, S_i is the simulated data, RMSE is the root mean square error, SD is the standard deviation, and z is the number of model parameters. When $R^2 = 1$, the simulated data perfectly match the observed data. A threshold of $R^2 = 0.65$ has been proposed in the literature to be the lower limit of valid goodness-of-fit (Moriasi et al. 2007, Ritter & Muñoz-Carpena 2013).

The 'best' model was then objectively selected as that which achieved the highest model performance (maximized the median R^2) while maintaining parsimony (minimizing median BIC) (Zuur et al. 2007). Note that although the same model structure (covariates) was used for all stations, each model was fit with local data; for example, the Stn 1 models were fit with data collected at Stn 1.

(5) Model evaluation

Model goodness-of-fit was evaluated using R^2 coupled with a block bootstrapping significance test (Politis & Romano 1994) that determined the confidence interval of each of the fitted models (Ritter & Muñoz-Carpena 2013). Although the upper and lower quantiles of the chl *a* distributions were modeled separately, the simulated results were recombined and ordered temporally to evaluate overall goodness-of-fit at each location.

Time series regression models are prone to having time-dependent errors (Helsel & Hirsch 2002), the presence of which results in a loss of effective degrees of freedom. Thus, it is prudent to evaluate model residuals for serial correlation and adjust error statistics accordingly. The Breusch-Godfrey test for evaluating autocorrelation in residuals of models that include an autoregressive explanatory variable (Asteriou & Hall 2011) was applied to each of the 56 models' residuals. The null hypothesis of the Breusch-Godfrey test is that the residuals have no autoregressive structure over the window of considered lags (in this case, 12 mo). For models that did not pass the Breusch-Godfrey test at an alpha level of 0.05, the residuals were fit with autoregressive models of order one (AR(1)) and the autocorrelation functions of their residuals were plotted. When the AR(1) model effectively removed the autocorrelation, as evidenced by insignificant values in the autocorrelation function plots, the standard errors of the coefficients and associated p-values were recalculated using an effective sample size (N_e; Eq. 4) that accounts for the loss of effective degrees of freedom resulting from the presence of residual autocorrelation (Mitchell et al. 1966, Santer et al. 2000):

$$N_e \approx N \frac{1 - r_1}{1 + r_1} \quad (4)$$

where r_1 is the residual autocorrelation coefficient of the first lag (1 mo); this correction is only adequate when model residuals have an AR(1) structure.

(6) Relative importance of explanatory variables

Explanatory variable importance was quantified using 2 metrics: average semipartial R^2 (Lindeman et al. 1980) and regression coefficient values. By locally fitting the 56 models with the same set of explanatory variables, direct comparisons of each explanatory variable's relative importance in describing chl *a* dynamics could be made across locations.

Semipartial R^2 quantifies an explanatory variable's individual contribution to the total variance explained by the model; the greater the variance explained by an explanatory variable, the greater its semipartial R^2 value, and the greater its importance. The semipartial R^2 values of all explanatory variables included within the model sum to the model's R^2 if the variables are orthogonal. Semipartial R^2 values associated with each explanatory variable can vary

as a function of the order in which explanatory variables are added to the model, which can bias the results. Average semipartial R^2 addresses this potential source of bias by calculating semipartial R^2 values for every possible explanatory variable order, and averaging the resulting vector of values.

The regression coefficient values of the quantile models were also evaluated as measures of relative importance. Coefficient magnitudes and semipartial R^2 values provide similar information with regards to importance of the covariates, but with differing interpretability. Semipartial R^2 values quantify the contribution of individual explanatory variables in terms of fraction of total explained variance, which can be interpreted in both relative and absolute terms; coefficient values can only be evaluated relative to one another. Because semipartial R^2 values are non-negative, they give no indication regarding relationship directionality (positive or negative) between explanatory variables and phytoplankton biomass, whereas coefficient values do. Therefore, when evaluated together, coefficient and semipartial R^2 values provide a complete and complementary picture of relative importance, absolute importance, and relationship directionality.

Coefficient and semipartial R^2 values were mapped at each of the station locations and spatially interpolated using inverse distance weighting to visualize each explanatory variable's importance under non-bloom and bloom conditions across the bay.

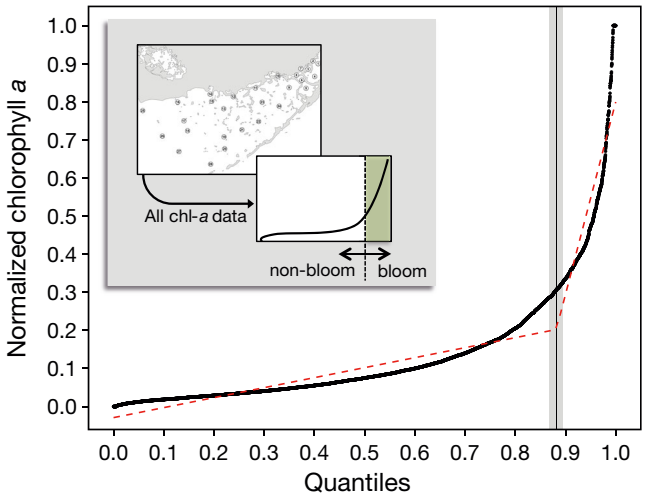

Fig. 2. Empirical cumulative distribution function (points) of normalized chlorophyll *a* (chl *a*) data from all 28 stations, and fitted piecewise linear curve (dashed red line). The curve break and its 95% confidence interval (break = 0.88 [0.87, 0.90]) are shown by the vertical black line and surrounding gray area, respectively. The inset depicts the supporting methodology and rationale

Software

Data management and analysis were performed in R (R Core Team 2015); specifically, the relaimpo package (Grömping 2006), SiZeR package (Sonderegger et al. 2009), gstat package, and lm function were employed for average semipartial R^2, piecewise linear regression, inverse distance weighting, and multiple linear regression calculations, respectively. Spatial data were plotted using functions in the raster and maptools packages. Quantification of R^2 confidence intervals using block bootstrapping was performed with the FITEVAL software package (Ritter & Muñoz-Carpena 2013) in MATLAB (The MathWorks Inc 2015). See Supplement 2 at www.int-res.com/articles/suppl/m567p057_supp2.zip for sample code.

RESULTS

Bloom threshold

The 0.88 quantile, with a 95% confidence interval of [0.87, 0.90], was identified as the breakpoint in the piecewise linear curve of the bay-wide chl *a* distribution (Fig. 2), thus also making it the threshold separating non-bloom from bloom conditions. This quantile threshold corresponded to station-specific chl *a* concentrations ranging from 0.86 to 7.70 µg l^{-1} (Table 1), with the majority of the threshold values falling below 2 µg l^{-1} (Fig. S2). To visualize the separation of bloom and non-bloom conditions against actual observations, the thresholds were plotted against chl *a* data (Fig. 3, Fig. S3). These plots confirmed that the quantile threshold successfully separated bloom events from non-bloom conditions across locations with varying ecologies.

Blooms by region

When evaluating the frequency of blooms across each region and year (Fig. 4), prevalent spatial and temporal patterns emerged. The longest-lasting bloom occurred in the Northeast Bay in 2006, and persisted for most of the year. Prior to 2006, blooms in the Northeast Bay, when present, typically lasted for less than 2 mo. Similarly, blooms in the remaining 4 regions of the bay generally endured for 3 mo or less. The East, North Central, and South Central Bay were similar in temporal structure, and characterized by strong bloom years in 1993, 1994, 1999, and 2006, and relatively mild bloom years from 2001 to 2004.

Table 1. Bloom (B) and non-bloom (NB) model parameters, semipartial R^2, and overall R^2 values for each station. Asterisks indicate significant differences from 0 (*p < 0.10, **p < 0.05, ***p < 0.01). Qtl: quantile; BT: bloom threshold (µg chl *a* l^{-1}); µ: level factor (µg chl *a* l^{-1}); chl *a*: antecedent chl *a*; T: water temperature; TN: total nitrogen; TP: total phosphorus; turb: turbidity; sal: salinity

Stn	Qtl	Multiple linear regression parameters								Semipartial R^2						R^2
		BT	µ	β_{chla}	β_T	β_{TN}	β_{TP}	β_{turb}	β_{sal}	R^2_{chla}	R^2_T	R^2_{TN}	R^2_{TP}	R^2_{turb}	R^2_{sal}	[95% CI]
1	B	1.31	0.048	0.375***	0.211	−0.121	−0.267	1.365***	0.118	0.213	0.015	0.004	0.013	0.238	0.018	0.828
	NB		0.002	0.353***	0.012	0.025**	0.054*	0.107***	0.009	0.261	0.006	0.02	0.034	0.073	0.001	[0.717, 0.863]
2	B	1.17	−0.05	0.405*	0.022	0.379	0.089	1.339***	0.286	0.222	0.02	0.017	0.022	0.243	0.069	0.853
	NB		0.031**	0.325***	0.009	0.006	0.032	0.109***	−0.002	0.187	0.001	0.005	0.011	0.079	0	[0.610, 0.898]
3	B	1.37	0.094	0.353	0.009	−0.206	0.091	0.534**	0.225	0.234	0.024	0.02	0.04	0.263	0.08	0.878
	NB		−0.002	0.459***	0.02**	0.016	0.044	0.02	0.003	0.318	0.02	0.015	0.036	0.007	0.002	[0.736, 0.908]
4	B	1.62	0.085	0.357	−0.035	0.265	−0.087	0.37	0.199	0.204	0.022	0.027	0.01	0.1	0.032	0.809
	NB		−0.013	0.43***	0.033*	−0.008	0.117	0.089	0.026	0.296	0.021	0.002	0.031	0.004	0.023	[0.571, 0.863]
5	B	1.57	−0.191	0.303	0.074	0.339	0.079	0.911*	0.313	0.144	0.01	0.04	0.002	0.135	0.027	0.815
	NB		0	0.444***	0.016	0.01	0.059	0.148***	0.008	0.344	0.003	0.012	0.012	0.083	0.001	[0.719, 0.853]
6	B	1.22	0.32**	0.097	−0.43**	−0.098	0.156	0.289	0.35*	0.154	0.198	0.006	0.059	0.139	0.111	0.823
	NB		0.004	0.289***	0.024***	0.015**	0.003	0.169***	−0.017**	0.186	0.034	0.048	0.014	0.081	0.07	[0.602, 0.877]
7	B	1.23	0.268	0.364	0.091	−0.25	0.527	−0.011	−0.269	0.194	0.019	0.045	0.175	0.017	0.036	0.752
	NB		0.049***	0.034	−0.005	0.014	0.036	0.143***	0.05***	0.018	0.004	0.008	0.01	0.122	0.126	[0.620, 0.802]
8	B	1.50	0.345*	−0.121	−0.226	−0.119	0.064	0.306*	0.588***	0.07	0.042	0.025	0.002	0.092	0.241	0.780
	NB		0.034*	0.264***	0.04**	0	0.029	0.072*	−0.028*	0.132	0.026	0.012	0.012	0.022	0.043	[0.568, 0.857]
9	B	0.86	0.571*	0.127	0.332	−0.485*	−0.27	−0.039	0.044	0.007	0.036	0.168	0.024	0.012	0.013	0.688
	NB		0.026	0.168***	0.017	0.096**	0.038	0.25**	0.009	0.095	0.002	0.056	0.001	0.054	0.004	[0.611, 0.763]
10	B	1.99	0.58***	0.087	0.128	−0.1	0.216	0.225	−0.212	0.013	0.035	0.045	0.064	0.121	0.045	0.694
	NB		0.096**	0.249***	0.036	−0.001	0.17**	0.705***	−0.145***	0.127	0.003	0.007	0.054	0.106	0.075	[0.562, 0.783]
11	B	0.92	0.615**	0.142	−0.185	−0.005	−0.068	−0.017	−0.122	0.061	0.067	0.002	0.006	0.001	0.01	0.656
	NB		0.084**	0.308***	0.066**	0.031	−0.031	0.034	−0.1**	0.198	0.02	0.019	0.002	0.015	0.07	[0.531, 0.732]
12	B	5.15	0.64***	−0.057	0.02	−0.087	0.369**	0.035	−0.081	0.062	0.008	0.014	0.283	0.009	0.057	0.856
	NB		−0.109***	0.252***	0.095**	0.134***	0.146***	0.444***	0.045	0.231	0.016	0.117	0.096	0.17	0.006	[0.783, 0.892]
13	B	5.05	0.785***	−0.142	−0.365	0.016	−0.146	1.092	−0.2	0.013	0.146	0.026	0.008	0.07	0.066	0.753
	NB		−0.032	0.27***	0.057	0.094*	0.133**	0.16**	0.006	0.151	0.007	0.074	0.117	0.055	0.006	[0.643, 0.821]
14	B	7.70	0.645***	−0.473**	−0.065	−0.27	−0.088	0.66**	−0.424**	0.061	0.003	0.05	0.007	0.097	0.222	0.750
	NB		0	0.222***	0.063***	0.025	0.174***	−0.017	−0.037	0.128	0.022	0.077	0.187	0.017	0.046	[0.642, 0.827]
15	B	6.79	0.823***	−0.39*	−0.25	−0.114	−0.171	0.434	−0.288*	0.067	0.086	0.041	0.014	0.055	0.14	0.754
	NB		−0.011	0.143***	0.051*	0.035	0.301***	0.038	−0.03	0.078	0.007	0.102	0.241	0.027	0.011	[0.662, 0.813]
16	B	5.45	0.426*	−0.01	0.27	0.032	0.559	−0.088	−0.38	0.007	0.031	0.015	0.142	0.028	0.075	0.71
	NB		0.111***	0.178***	0.037	0.058	0.066	0.199***	−0.094*	0.087	0.004	0.019	0.039	0.079	0.019	[0.598, 0.786]
17	B	3.31	0.309	0.112	0.241	−0.084	0.596	−0.231	−0.528	0.092	0.02	0.008	0.308	0.015	0.171	0.846
	NB		0.04	0.033	0.035	0.091	0.118	0.096	−0.085	0.025	0.01	0.085	0.13	0.084	0.063	[0.768, 0.899]
18	B	3.01	0.389*	0.153	−0.164	−0.086	0.523	−0.446	0.116	0.022	0.059	0.004	0.096	0.062	0.006	0.808
	NB		0	0.136***	0.054***	0.073***	0.135***	0.687***	−0.061**	0.124	0.013	0.078	0.095	0.22	0.027	[0.723, 0.855]
19	B	3.29	0.341*	−0.193	−0.047	−0.024	0.247	0.481***	0.01	0.061	0.041	0.009	0.123	0.338	0.013	0.846
	NB		−0.015	0.133***	0.032	0.059**	0.11***	0.243***	−0.004	0.1	0.008	0.046	0.088	0.14	0.004	[0.777, 0.912]
20	B	1.99	0.216	−0.105	0.253	0.126	0.704**	−0.172	−0.069	0.03	0.058	0.011	0.273	0.012	0.024	0.831
	NB		−0.043**	0.139***	0.062**	0.11***	−0.005	0.292***	0.002	0.099	0.016	0.047	0.007	0.171	0.003	[0.755, 0.883]
21	B	2.12	0.038	0.11	−0.092	−0.023	0.803***	0.135	0.232	0.041	0.014	0.022	0.455	0.257	0.023	0.884
	NB		−0.001	0.205***	0.031*	0.046**	0.01	0.067***	0.008	0.156	0.011	0.051	0.006	0.038	0.002	[0.793, 0.934]
22	B	1.31	0.441*	−0.066	−0.142	−0.04	0.475	0.036	0.013	0.003	0.034	0.003	0.068	0.009	0.01	0.718
	NB		0.012	0.196***	0.03	0.031	0.017	0.071	0.008	0.177	0.019	0.033	0.003	0.004	0.002	[0.627, 0.778]
23	B	0.88	0.265	0.143	−0.09	0.116	0.682	0.399	−0.025	0.051	0.02	0.015	0.168	0.195	0.028	0.741
	NB		0.051**	0.283***	0.017	0.07**	−0.04	0.142**	−0.031	0.193	0.006	0.034	0.003	0.026	0.014	[0.618, 0.816]
24	B	0.87	0.256***	0.207*	0.135	−0.286***	0.108	0.46***	0.168	0.02	0.023	0.116	0.076	0.43	0.043	0.764
	NB		0.034	0.24***	−0.004	0.016	−0.017	0.212***	0.028	0.12	0.01	0.007	0.001	0.099	0.003	[0.630, 0.879]
25	B	4.49	0.399**	−0.022	0.43	0.026	0.265	0.171	−0.39**	0.006	0.033	0.008	0.022	0.116	0.159	0.693
	NB		0.158***	0.034	0.059	0.04	0.02	0.234***	−0.124***	0.008	0.01	0.005	0.03	0.114	0.053	[0.577, 0.788]
26	B	4.12	0.356	−0.141	0.293	−0.009	0.575	0.29	−0.395	0.009	0.016	0.001	0.041	0.076	0.046	0.675
	NB		0.118***	0.117**	−0.025	0.052	−0.152*	0.267***	−0.064**	0.051	0.018	0.017	0.018	0.09	0.054	[0.582, 0.738]
27	B	2.09	−0.105	0.154	0.215	0.47***	−0.845	0.603***	−0.018	0.034	0.018	0.134	0.124	0.324	0.054	0.808
	NB		0.03***	0.096***	0.006	0	−0.108***	0.192***	−0.015	0.064	0.005	0.001	0.021	0.038	0.023	[0.554, 0.884]
28	B	1.57	0.248**	−0.012	0.411***	0.241*	0.709***	−0.656***	−0.233*	0.018	0.145	0.112	0.147	0.112	0.024	0.792
	NB		0.05**	0.157***	0.063***	0.042	0.028	0.113**	−0.084***	0.094	0.009	0.009	0.001	0.024	0.031	[0.690, 0.859]

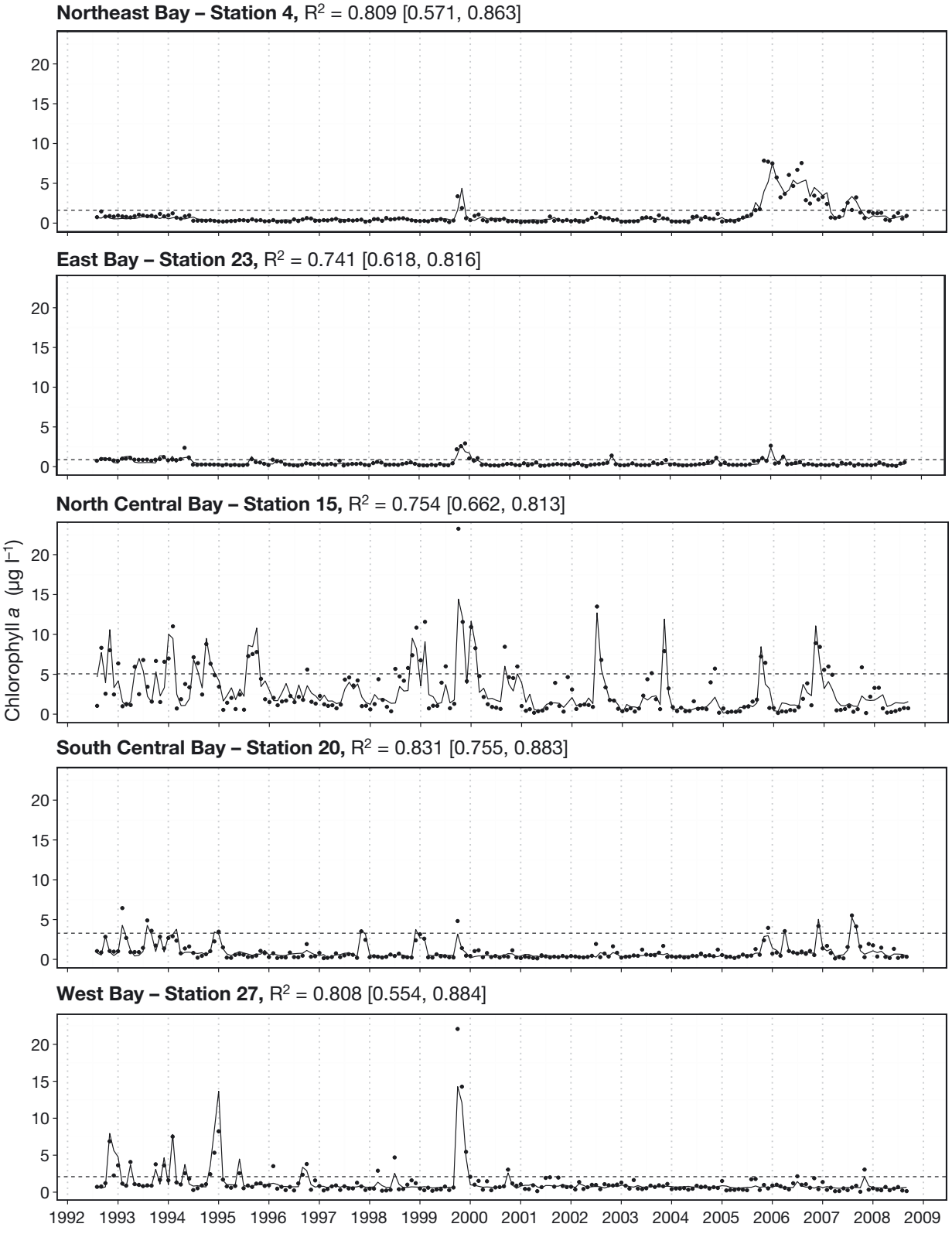

Fig. 3. Chlorophyll *a* concentration. Observed (points) and modeled (solid line) data from representative sites of each region in Florida Bay; station-specific bloom thresholds shown as horizontal dashed lines. Coefficients of determination (R^2) and corresponding confidence intervals are included

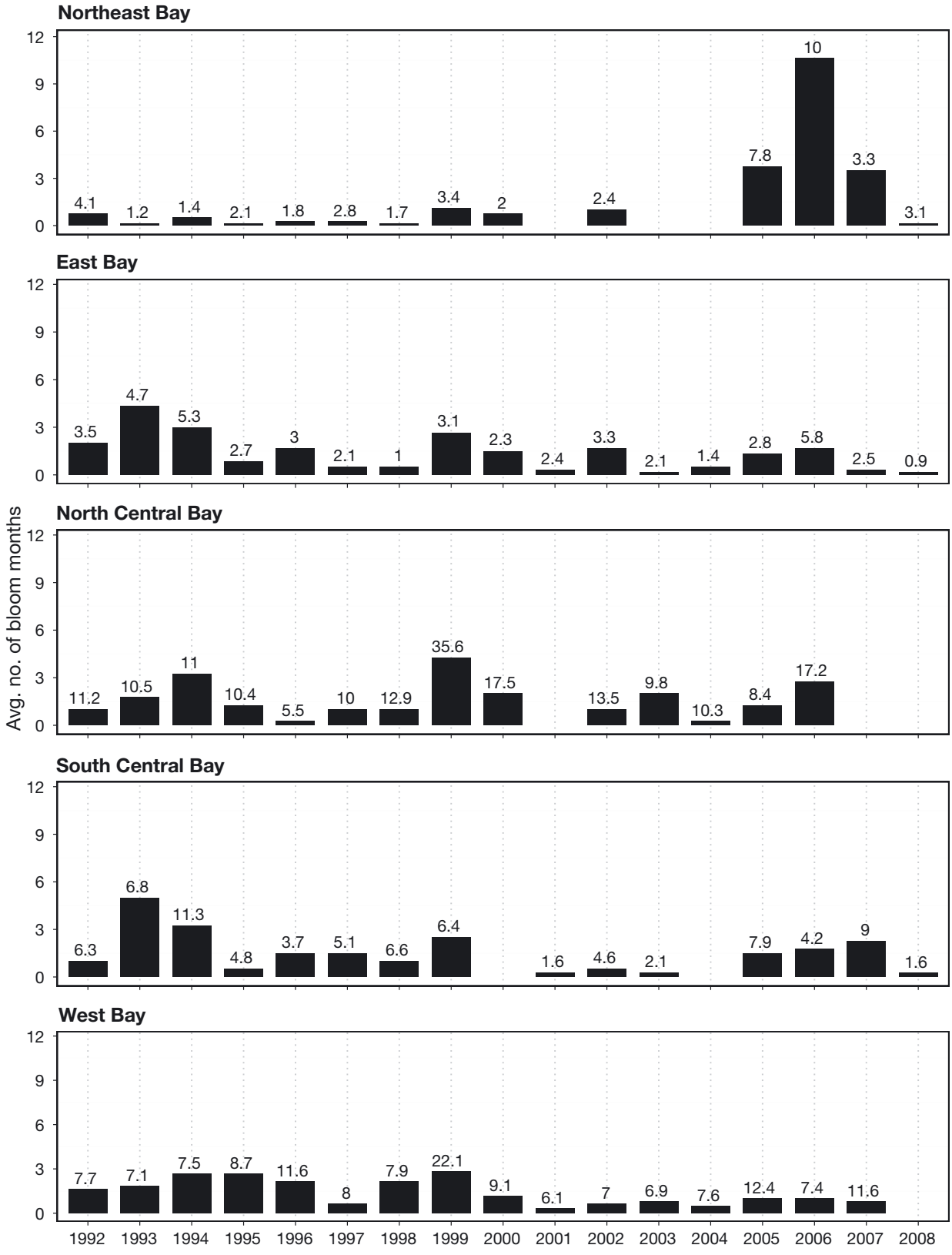

Fig. 4. Average number of bloom months per year and region (calculated as total number of regional monthly bloom observations, divided by the number of stations within the region). Yearly chlorophyll *a* maxima (µg l^{-1}) are shown above each bar

Though these regions were similar in terms of the average number of bloom months per year, their chl *a* concentrations greatly differed. The greatest chl *a* concentrations occurred in the North Central Bay; the maximum chl *a* concentration in this dataset was recorded in the North Central Bay in 1999 at a value of 35.6 µg l^{-1} (Fig. 4). In contrast, the maximum recorded chl *a* concentration in the longstanding 2007 bloom of the Northeast Bay measured 10 µg l^{-1}. Bloom temporality in the West Bay was unlike that observed in the other bay regions; the blooms persisted for approximately 1 to 2 mo each year in the West Bay, with the periods of 1992–1999 and 2000–2008 tending more towards 2 and 1 bloom month(s) per year, respectively. This regularity was more indicative of natural blooms, which contrasted with the irregularity of bloom frequency in the other regions. With the exception of the Northeast Bay, bloom duration throughout the bay generally declined over the study period; notably, no blooms were observed in the last 2 years of the study period (2007–2008) in the North Central Bay.

Selection of model variables

All of the considered water quality variables were non-collinear (maximum VIF = 4.64; Table S1) and included in the model screening process. After evaluating all possible candidate explanatory variable combinations for model performance and parsimony, the final set of candidate explanatory variables included all considered variables: total nitrogen (*TN*), antecedent chlorophyll *a* ($chla_{t-1}$), total phosphorus (*TP*), water temperature (*T*), turbidity (*turb*), and salinity (*sal*). Antecedent chlorophyll *a* was defined as chl *a* from the previous month, or 'lagged' chl *a*. For a summary of model screening results, see Fig. S4 and Table S2.

Spatial variation in the medians of each of these variables for the lower (non-bloom) and upper (bloom) quantiles is shown in Fig. 5. Median chl *a* concentrations under bloom conditions generally increased from less than 4 µg l^{-1} in the East/Northeast Bay to greater than 4 µg l^{-1} in the West Bay, with the exception of a strong peak in the North Central Bay in excess of 10 µg l^{-1} (Fig. 5A). For non-bloom conditions, median chl *a* concentrations showed a modest decline from less than 1 µg l^{-1} in the Central and East/Northeast Bay to 0.5–2 µg l^{-1} in the West and North Central Bay (Fig. 5B).

Median water temperatures under bloom conditions varied from upwards of 28°C in the North Central and East Bay regions, to less than 25°C in parts of the East and South Central Bay (Fig. 5C). In contrast, median water temperatures during non-bloom conditions were spatially uniform and ranged from 26 to 27°C throughout Florida Bay (Fig. 5D).

Median TN concentrations under bloom conditions were highest in the Central and parts of the East Bay with values in excess of 0.8 mg l^{-1}, peaking in the North Central Bay at greater than 1.2 mg l^{-1} (Fig. 5E). To the east and west of the central region, median TN concentrations declined to less than 0.8 mg l^{-1}, with the lowest values on the western boundary of the bay. The same general spatial pattern of median TN levels was observed under non-bloom conditions, but at lower levels (Fig. 5F).

Median TP concentrations under bloom conditions generally increased from less than 0.02 mg l^{-1} in the East/Northeast Bay to greater than 0.02 mg l^{-1} in the West/South Central Bay, with a strong peak in the North Central/North West Bay in excess of 0.035 mg l^{-1} (Fig. 5G). For non-bloom conditions, median TP concentrations showed an east to west gradient, from less than 0.01 mg l^{-1} in the East/Northeast Bay to around 0.015 mg l^{-1} in the West Bay with a peak in the North Central Bay near 0.02 mg l^{-1} (Fig. 5H).

Median turbidity levels under bloom conditions showed a spatial pattern similar to that of median TP concentrations, with values less than 7 nephelometric turbidity units (NTU) in the Northeast and South Central Bay to greater than 7 NTU in the West Bay and parts of the North Central Bay; median turbidity values were greatest in the northwestern region of the West Bay, where values exceed 15 NTU (Fig. 5I). For non-bloom conditions, median turbidity levels were generally below 5 NTU through most of the bay, with values below 2 NTU in the Northeast Bay and in the South Central Bay near major inlets to the Atlantic Ocean in the southern Florida Keys (Fig. 5J).

Median salinities during blooms (Fig. 5K) were, on average, less than those during non-blooms (Fig. 5L). Median salinity was highest in the West Bay, where values ranged from about 27 to 35 PSU between blooms and non-blooms, respectively. Median salinity was lowest in the East Bay, particularly on its northern shore; within the East Bay, salinity ranged north-to-south from less than 10 PSU to greater than 20 PSU during bloom and non-bloom conditions.

Bay-wide quantile model

The multiple linear regression model used in this study to describe key relationships between phytoplankton biomass (as chl *a*) and the aforementioned

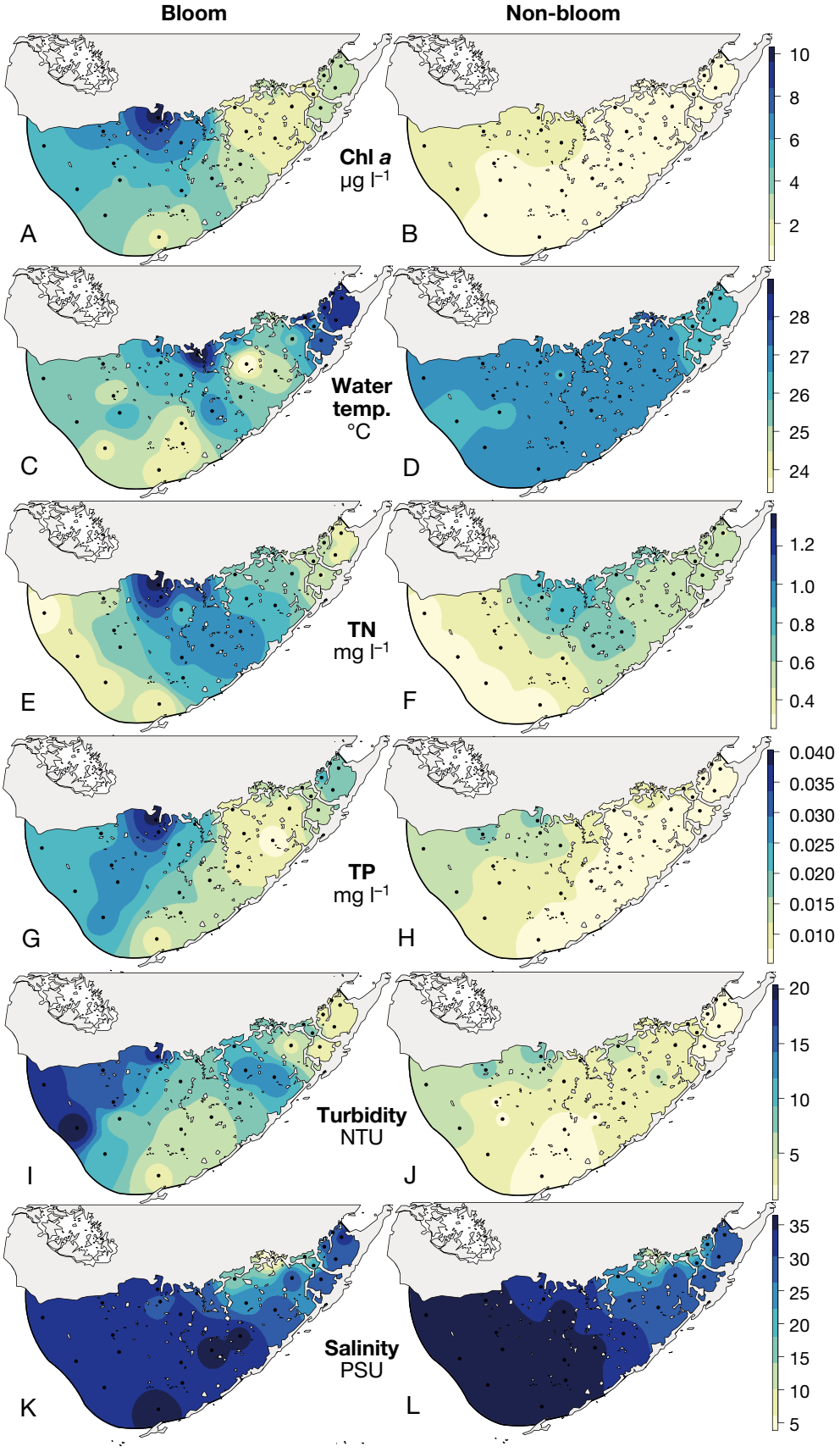

Fig. 5. Bloom (left column) and non-bloom (right column) quantile medians of observed (A,B) chlorophyll *a* (chl *a*; µg l^{-1}), (C,D) water temperature (°C), (E,F) total nitrogen (TN; mg l^{-1}), (G,H) total phosphorus (TP; mg l^{-1}), (I,J) turbidity (NTU), and (K,L) salinity (PSU). Observed values were spatially interpolated between the 28 stations

covariates is described by Eq. (5), where k denotes the station, q represents the quantile (upper or lower), μ is the level factor, and the βs are coefficient values:

$$chla_{q,k} = \mu_{q,k} + \beta_{chla,q,k} chla_{(t-1),k} + \beta_{T,q,k} T_k + \beta_{TN,q,k} TN_k + \beta_{TP,q,k} TP_k + \beta_{turb,q,k} turb_k + \beta_{sal,q,k} sal_k \quad (5)$$

Each model suite was separately fit to the upper 12% and lower 88% of the chl *a* data at each station. This produced a total of 28 lower quantile models and 28 upper quantile models; all of the models had the same explanatory variables, but with different coefficients as each model was fit with local data (Table 1).

Of the 56 models, 21 had residuals with non-zero autocorrelation over a 12-mo window at a significance level of 0.05 (Table S3), and an approximately AR(1) structure (Fig. S5). The p-values of these models' coefficients were adjusted using the effective sample size to account for the residuals' time dependency.

Overall, the models performed well in reproducing chl *a* values from non-bloom and bloom conditions. The bay-wide average R^2 of all locations was 0.78, with a range of 0.66 (Stn 11) to 0.88 (Stn 21). R^2 values with confidence intervals for all 28 stations are shown in Table 1. Representative simulated data series from each of the 5 regions of Florida Bay are shown in Fig. 3 (solid lines).

Spatial patterns of model coefficients and semipartial R^2

Spatial patterns of explanatory variable importance under bloom and non-bloom conditions are summarized in Table 1 and Fig. 6. Under bloom conditions, there was a positive relationship between phytoplankton biomass and antecedent chl *a* in the Northeast, East, and West Bay, and a mildly negative relationship in the North and South Central Bay (Fig. 6C). The semipartial R^2 results showed that the strength of this relationship was at its peak in the Northeast Bay, and weak elsewhere (Fig. 6A). The spatial pattern in the importance of antecedent chl *a* under non-bloom conditions was similar to that during bloom conditions, but with greater semipartial R^2 values, consistently positive coefficients, and decreasing importance going westward from the Northeast Bay (Fig. 6B,D).

Coefficient values revealed that phytoplankton biomass and water temperature were positively related throughout most of the bay under bloom conditions, with some stations in the North Central Bay and along the northern shore of the East Bay being parameterized by negative coefficients (Fig. 6G); the semipartial R^2 values revealed that water temperature was mostly of minor to moderate importance in the central region of the bay, and negligible elsewhere (Fig. 6E). Under non-bloom conditions, water temperature was an inconsequential descriptor of phytoplankton biomass (Fig. 6F,H).

During bloom conditions, relationships between phytoplankton biomass and TN ranged from mildly negative in the East Bay and northern shore of the North Central Bay, to slightly positive in the southwestern part of the West and Northeast Bay, to negligible in the remaining areas of the bay (Fig. 6K). Overall, TN explained a relatively small fraction of phytoplankton biomass variance under bloom conditions (Fig. 6I). During non-bloom conditions, the relationships between phytoplankton biomass and TN were minor (Fig. 6J) and characterized by inappreciable coefficient values (Fig. 6L). In contrast, under bloom conditions, TP explained considerable phytoplankton biomass variance at many locations, particularly those in the North and South Central Bay, and stations neighboring these regions in the West and East Bay (Fig. 6M). In areas where the relationship between TP and phytoplankton biomass during blooms was the strongest, coefficient values were positive; in other areas where TP explained relatively less phytoplankton biomass variance, coefficient values ranged from strongly to mildly negative (Fig. 6O). Under non-bloom conditions, the relationship between phytoplankton biomass and TP was greatest in the North Central Bay, and mildly to negligibly important elsewhere in the bay (Fig. 6N); coefficient values were positive in the North Central Bay, and predominantly negligible elsewhere (Fig. 6P).

Semipartial R^2 values characterizing the relationship between turbidity and phytoplankton biomass during bloom conditions highlighted a great deal of variability across the bay; each region included stations whereat turbidity was either a strong or weak descriptor of phytoplankton biomass (Fig. 6Q). Coefficient values parameterizing turbidity under bloom conditions were predominantly positive, but a band of negative values was distinctly present along the eastern boundary of the West Bay (Fig. 6S). During non-bloom conditions, turbidity was a moderately important descriptor of phytoplankton biomass (Fig. 6R), particularly in the central region and the West Bay, and was consistently parameterized by positive coefficient values (Fig. 6T).

Salinity was predominantly of negligible importance during non-bloom conditions, but explained a

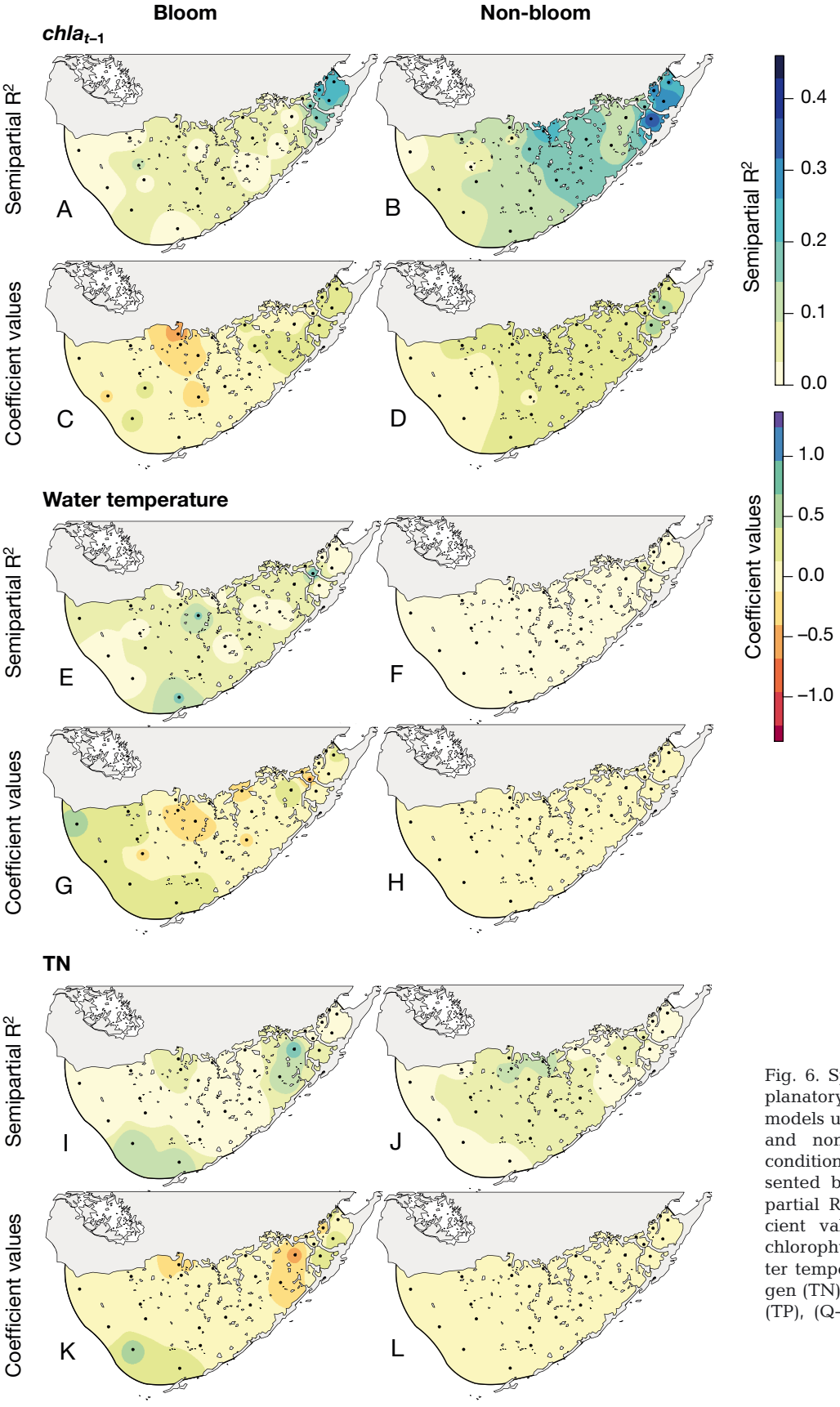

Fig. 6. Spatial importance of explanatory variables in the quantile models under bloom (left column) and non-bloom (right column) conditions. Importance is represented by distributions of semipartial R^2 and regression coefficient values: (A–D) antecedent chlorophyll *a* (*chla*$_{t-1}$), (E–H) water temperature, (I–L) total nitrogen (TN), (M–P) total phosphorus (TP), (Q–T) turbidity, and (U–X) salinity

(continued on next page)

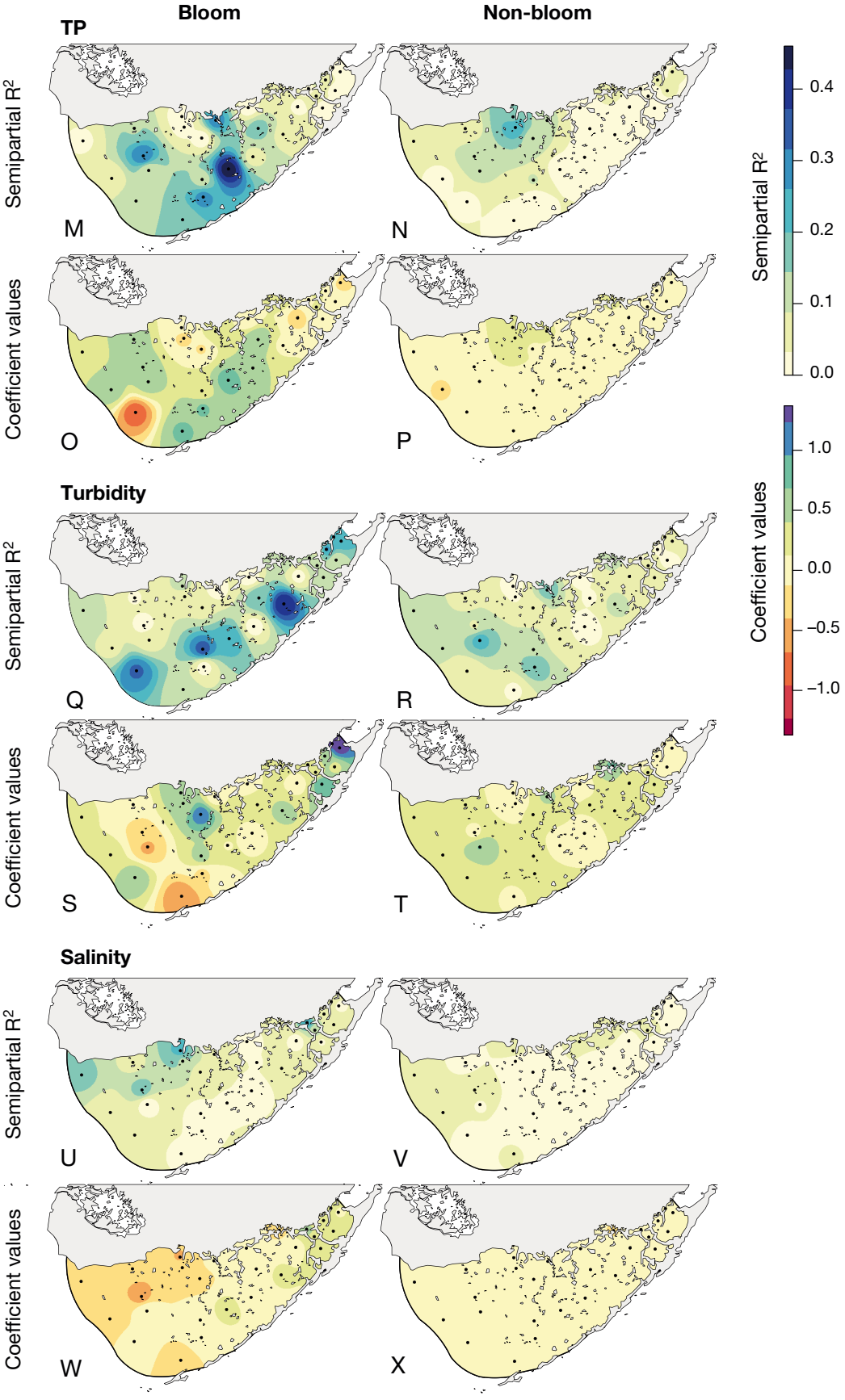

Fig. 6 (continued)

small fraction of phytoplankton biomass variance in the West Bay (Fig. 6V,X). Conversely, salinity was an important descriptor of blooms in the North Central and West Bay (Fig. 6U). In these regions, where salinity played an influential role on bloom biomass, the corresponding coefficient values were negative (Fig. 6W).

DISCUSSION

The results of the modified quantile regression analysis of Florida Bay revealed regional differences in the importance of water quality covariates associated with phytoplankton biomass (i.e. as chl *a*) under bloom and non-bloom states, including antecedent chl *a*, water temperature, TN, TP, turbidity, and salinity. From the perspective of phytoplankton structure and function, the non-bloom state includes periods of bloom initiation and biomass expansion, which are strongly affected by the availability of growth-supporting resources, such as nutrients and light, and the presence of seed populations (Reynolds 2006). The bloom state represents a period of biomass climax and stationary state, which is often associated with nutrient limitation, diminished growth rates, self-shading of light, and increased proportion of senescent/diseased cells (Reynolds 2006), as well as enhanced potential for top-down control due to increases in zooplankton grazer abundances (Ward et al. 2014). The findings of the model analyses for bloom and non-bloom states are discussed below; note that the mechanisms offered as possible drivers of the statistical results produced herein are hypothetical, and confirmation of their validity requires further testing through mechanistic modeling or controlled experiments.

Non-bloom conditions

Antecedent chl *a* was a positive predictor of non-bloom phytoplankton biomass throughout the bay, which demonstrates the importance of this autoregressive variable and reflects how increases in biomass are progressive during the early and exponential stages of growth and expansion. In the East and Northeast Bay, the high degree of importance of this autoregressive variable relative to the other considered explanatory covariates highlights the more oligotrophic character of these regions, which diminishes the temporal longevity and magnitude of shifts in nutrient availability, and dampens the dynamic scale of biomass variability (Reynolds 2006). Non-bloom phytoplankton biomass in regions outside of the East and Northeast Bay were also described by TP, TN, and turbidity. The coefficient values in the 28 non-bloom models were all positive, with only one exception for Stn 26 in the West Bay. Combined, the results indicate that: (1) non-bloom phytoplankton biomass increases when the biomass from the prior month is relatively elevated, (2) non-bloom phytoplankton biomass in southern, central and northern Florida Bay increases in response to elevated TP concentrations, while in the western bay, biomass responds more strongly to increases in TN, and (3) increases in turbidity in the southern, central and western regions of the bay relate to increases in non-bloom biomass.

In the North Central Bay, the importance of TP under non-bloom conditions reflects the overriding importance of phosphorus as a descriptor of phytoplankton growth in this region (Fourqurean et al. 1993, Boyer et al. 1999, Rudnick et al. 1999, Glibert et al. 2004). The more moderate importance of TN may be explained in relationship to TN-enriched runoff from the bordering watersheds of the Florida Everglades (Fourqurean et al. 1993, Rudnick et al. 1999). The relative importance of phosphorus and nitrogen limitation varies by region, with greater potential for nitrogen limitation in the western bay and more prominent phosphorus limitation in the central and eastern areas of the bay (Fourqurean et al. 1993, Rudnick et al. 1999, Glibert et al. 2004). The pattern of nutrient limitation is, in part, a product of relatively low inorganic and organic phosphorus concentrations in sources of loading from the Everglades into the central and eastern regions of the bay (Rudnick et al. 1999); in contrast, comparatively high inorganic and organic nitrogen levels, as well as dissolved organic carbon, from the Everglades may help to promote phytoplankton growth (Glibert et al. 2004, Boyer et al. 2006, Goleski et al. 2010). It has also been proposed that the dominance of major blooms in the North Central Bay by picoplanktonic cyanobacteria (Phlips et al. 1999) is in part a result of 2 key factors: (1) the ability of these species to compete effectively for phosphorus at low concentrations and take advantage of organic forms of nitrogen and phosphorus (Glibert et al. 2004, Boyer et al. 2006, Goleski et al. 2010), and (2) low rates of zooplankton grazing losses for picoplanktonic cyanobacteria compared to eukaryotic taxa (Glibert et al. 2004, Boyer et al. 2006, Goleski et al. 2010).

The positive relationship between turbidity and non-bloom phytoplankton biomass in Florida Bay

runs contrary to observations from some other ecosystems wherein increases in turbidity are associated with inhibition of phytoplankton growth as a result of corresponding decreases in water column light availability (Gameiro et al. 2011). However, due to the very shallow depths (i.e. <2 m) throughout Florida Bay, pelagic light availability appears to remain at levels that support phytoplankton growth (Phlips et al. 1995, Kelble et al. 2005), meaning that changes in turbidity do not necessarily create light-limiting conditions. There are several processes that could potentially underlie a positive relationship between turbidity and phytoplankton biomass, such as resuspension of sedimented algae (Carrick et al. 1993), and/or turbulence-driven injection of nutrient-rich porewater into the water column (Santschi et al. 1990, Lawrence et al. 2004). The latter process is particularly relevant in Florida Bay due to its calcium-carbonate-rich sediment deposits (Zhang et al. 2004), where nutrients are both adsorbed to the sediment and available in benthic porewaters (Santschi et al. 1990).

Water temperature was a largely insubstantial predictor of phytoplankton biomass overall, as was salinity. The water temperature result is not surprising considering the subtropical/tropical location of Florida Bay, where water temperatures exceed 25°C for most of the year and only occasionally drop below 20°C for short periods of time as a result of midwinter passage of cold fronts.

Bloom conditions

While predictors of non-bloom biomass provide insights into factors that support increases in phytoplankton biomass, the predictors associated with the bloom biomass subset of the data help to identify factors associated with the highest peaks in biomass.

A number of parameters were significant predictors of bloom biomass in one or more regions of Florida Bay, including turbidity, salinity, and TP, and, to a lesser extent, temperature, TN, and antecedent chl *a*.

From a bay-wide perspective, turbidity was the most broadly important descriptor of bloom phytoplankton biomass, primarily as a positive correlate. The mechanisms previously described to explain the positive turbidity–phytoplankton relationships under non-bloom conditions (i.e. porewater mixing, nutrient desorption and re-suspension of sedimented algae) also help to explain the turbidity–bloom relationship. The opposite trend of a negative turbidity–bloom relationship in parts of the West Bay may reflect difference sources of phytoplankton biomass in this location as compared to other parts of the bay. The openness of the West Bay to the Gulf of Mexico indicates that temporal dynamics of phytoplankton biomass in this region are driven by allochthonous biomass inputs from the southeastern gulf, and less by local autochthonous processes which dominate in the rest of the bay. For example, turbidity may induce light limitation of phytoplankton production in the deeper regions of the adjacent gulf, thereby indirectly influencing biomass in the West Bay. The importance of allochthonous influences on blooms in estuaries has been observed elsewhere (Phlips et al. 2012, Hart et al. 2015).

Salinity was inversely related to phytoplankton bloom biomass in the West and North Central Bay. Although elevated salinity can dampen biomass of stenohaline species (Reynolds 2006), the dominant bloom-forming taxa in Florida Bay, *Synechococcus* spp., are strongly euryhaline and therefore minimally impacted by hypersaline conditions observed in this region (Phlips & Badylak 1996, Phlips et al. 1999, Richardson 2009). Therefore, in the North Central Bay, hypersalinity alone is not expected to drive an appreciable reduction in bloom biomass. More likely, lower salinities reflect inputs of water and nutrients from local coastal watersheds, including the Everglades and the river-dominated estuaries of southwest Florida, which elevate bloom biomass potential. Phlips et al. (1999) noted this relationship during the strong cyanobacteria bloom period of 1993–1996 in the North Central Bay, where peak phytoplankton biomass levels often coincided with periods of declining salinity. A similar hypothetical explanation may extend to the West Bay, as phytoplankton blooms in the adjacent Gulf of Mexico can be enhanced by freshwater discharges from watersheds along the southwest coast of Florida (Heil et al. 2007, Boyer et al. 2009, Zhao et al. 2013), and, in turn, be imported into this region of the bay.

Water temperature was least important as a descriptor of phytoplankton biomass under bloom conditions in the West and East Bay, and of mostly mild importance elsewhere. Coefficient values parameterizing water temperature in bloom models were primarily positive, except along the northern shore of the North Central and East Bay. This implies that, in these areas, bloom biomass decreases as temperatures increase, whereas the inverse relationship is evident elsewhere in the bay. The negative temperature–bloom relationship could be explained by seasonality of rainfall, whereby blooms along the north-

ern shore decrease in response to greater freshwater runoff from the Everglades, and, consequently, greater hydrodynamic flushing. Furthermore, the temperature regime of Florida Bay does not preclude the formation of blooms in the winter season, as observed by Phlips et al. (1999).

The lack of consistent importance of TP as a significant positive predictor of bloom biomass in most of the bay except the south central region suggests that blooms, as defined by the data subset of peak biomass values in the 88% quantile, are not as closely aligned to nutrient factors as observed in the non-bloom state. It is important to keep in mind that the peak biomass achieved by blooms can be affected by a range of non-nutrient factors, such as grazing losses, sedimentation of phytoplankton cells, and flushing rates (i.e. export or dilution of biomass). In addition, bioavailable nutrients that initially drive the early stages of bloom initiation and expansion (i.e. included in the non-bloom state data sub-set defined in this study) can become depleted at peak bloom biomass levels, leading to declines in biomass potential, even though total nutrient concentrations in the water column may not be dramatically altered. By contrast, TP was a consistent positive bloom descriptor in the South Central Bay. Previous studies have shown that tidal exchange with the Gulf of Mexico delivers TP to this region (e.g. Fourqurean et al. 1993), which may in part help to explain the spatial pattern observed in the TP bloom results.

Though TN was of minimal or negligible importance in predicting bloom biomass throughout the bay, it was associated with negative coefficient values in the North Central and East Bay regions, meaning that an increase in TN was associated with a decrease in blooms. Since an increase in TN would not be expected to suppress phytoplankton growth during bloom conditions, this relationship provides further support for the previously proposed hypothesis of TN acting as a tracer of freshwater: while terrestrial runoff may provide nutrient subsidies during non-bloom conditions, study results suggest that terrestrial runoff may dampen phytoplankton biomass during blooms. Increased hydrodynamic flushing can negatively impact biomass, particularly during later stages of the bloom cycle, when growth rates are relatively low (Monsen et al. 2002).

Evaluated together, these results suggest the following: (1) the Northeast Bay's bloom phytoplankton biomass is autoregressive and minimally explained by additional descriptors included in this study, (2) factors that contribute to phytoplankton biomass during non-bloom conditions (antecedent chl *a*, water temperature, and TN) negatively influence bloom phytoplankton biomass in the North Central Bay, (3) pulses of TP in the South Central Bay and parts of the North Central and West Bay result in bloom increases, (4) turbidity positively influences bloom phytoplankton biomass in locations where it explains a large fraction of the phytoplankton biomass variance, but also dampens growth in regions where brackish and marine waters converge, and (5) increases in salinity prompt decreases in blooms in the West and North Central Bay.

CONCLUSIONS

The central goal of this study was to identify how spatial and temporal water quality variability differentially drives phytoplankton biomass during bloom and non-bloom conditions. Using a novel modification of quantile regression, bloom and non-bloom conditions were comparatively evaluated to calculate how spatiotemporal changes in environmental variability correlated to these phytoplankton biomass states. By regressing explanatory covariates against management-relevant quantiles of the response variable (bloom, non-bloom), this approach contrasted with traditional quantile regression, whereby explanatory variables are regressed against several narrow and arbitrary quantiles of the response variable. This analytical framework offered a straightforward and objective method for identifying a bloom threshold without having to select a reference system, as well as for comparing phytoplankton biomass dynamics across a diverse set of monitoring sites.

This new approach successfully identified water quality descriptors of both bloom and non-bloom phytoplankton conditions in Florida Bay, the site investigated in this analysis, and informed the development of data-driven hypotheses for future research regarding potential underlying mechanisms driving phytoplankton biomass dynamics in the bay. Human-driven changes to surface water flow from Central to South Florida, including the Everglades, over the span of a century have impacted the ecology of Florida Bay and contributed to phytoplankton blooms in this iconic ecosystem (Fourqurean & Robblee 1999, Rudnick et al. 2005). The minimal climatic forcing and highly variable phytoplankton biomass dynamics that characterize Florida Bay make this system a representative study site for analysis of bloom trends in low-latitude systems. Results from this study highlighted complicated relationships between nutrients and phytoplankton biomass, particularly in the North

Central Bay, and the widespread importance of turbidity, TP, and autoregressive chl *a* as correlates of bloom and non-bloom conditions. Beyond water quality drivers, further research should (1) address other processes known to influence phytoplankton biomass dynamics in Florida Bay, such as grazing by zooplankton (Goleski et al. 2010) and benthic filter feeders (Lynch & Phlips 2000, Peterson et al. 2006), which were not addressed in this study due to a lack of available long-term data, and (2) test hypotheses inspired by statistical findings herein, such as of the potential importance of non-nutrient (i.e. physical) factors as bloom drivers in the North Central Bay, and allochthonous inputs in the West Bay.

Though this study analyzed data solely from Florida Bay, the processes driving change in this system are broadly relevant to other bloom-affected estuarine systems, particularly those characterized by heterogeneous ecologies. Researchers and water quality managers in these settings will find the modified quantile regression methodology proposed herein readily applicable and useful for providing insights on bloom dynamics.

Acknowledgements. N.G.N. is supported by a National Science Foundation Graduate Research Fellowship under grant no. DGE-0802270. Data were provided by the SERC-FIU Water Quality Monitoring Network, which is supported by SFWMD/SERC Cooperative Agreement no. 4600000352 as well as EPA Agreement no. X7-96410603-3. R.M.C. acknowledges the support of the Florida Water Institute Faculty Fellowship. This work is supported by the USDA NIFA Hatch Project 1011481. The authors kindly thank David Kaplan and 3 anonymous reviewers for their thoughtful and constructive suggestions. The authors declare that there are no conflicts of interest.

LITERATURE CITED

Asteriou D, Hall SG (2011) Applied econometrics. Palgrave Macmillan, New York, NY

Boesch DF, Armstrong NE, D'Elia CF, Maynard NG, Paerl HW, Williams SL (1993) Deterioration of the Florida Bay ecosystem: an evaluation of the scientific evidence. Report to the Interagency Working Group on Florida Bay, Department of the Interior, National Park Service, Washington, DC

Boyer JN, Briceño HO (2007) South Florida Coastal Water Quality Monitoring Network FY2006 Cumulative Report to the South Florida Water Management District. Southeast Environmental Research Center, Florida International University. http://serc.fiu. edu/wqmnetwork/

Boyer JN, Fourqurean JW, Jones RD (1997) Spatial characterization of water quality in Florida Bay and Whitewater Bay by multivariate analyses: zones of similar influence. Estuaries 20:743–758

Boyer JN, Fourqurean JW, Jones RD (1999) Seasonal and long-term trends in the water quality of Florida Bay (1989-1997). Estuaries 22:417–430

Boyer JN, Dailey SK, Gibson PJ, Rogers MT, Mir-Gonzalez D (2006) The role of dissolved organic matter bioavailability in promoting phytoplankton blooms in Florida Bay. Hydrobiologia 569:71–85

Boyer JN, Kelble CR, Ortner PB, Rudnick DT (2009) Phytoplankton bloom status: Chlorophyll *a* biomass as an indicator of water quality condition in the southern estuaries of Florida, USA. Ecol Indic 9:S56–S67

Briceño HO, Boyer JN (2010) Climatic controls on phytoplankton biomass in a sub-tropical estuary, Florida Bay, USA. Estuaries Coasts 33:541–553

Burd AB, Jackson GA (2002) An analysis of water column distributions in Florida Bay. Estuaries 25:570–585

Butler MJ, Hunt JH, Herrnkind WF, Childress MJ and others (1995) Cascading disturbances in Florida Bay, USA: cyanobacteria blooms, sponge mortality, and implications for juvenile spiny lobsters *Panulirus argus*. Mar Ecol Prog Ser 129:119–125

Cade BS, Noon BR (2003) A gentle introduction to quantile regression for ecologists. Front Ecol Environ 1:412–420

Carrick HJ, Aldridge FJ, Schelske CL (1993) Wind influences phytoplankton biomass and composition in a shallow, productive lake. Limnol Oceanogr 38:1179–1192

Carvalho L, Mcdonald C, de Hoyos C, Mischke U and others (2013) Sustaining recreational quality of European lakes: minimizing the health risks from algal blooms through phosphorus control. J Appl Ecol 50:315–323

CERP (2005) Comprehensive Everglades Restoration Plan. 2005 Report to Congress. US Army Corps of Engineers and US Department of the Interior

Cloern JE (1982) Does the benthos control phytoplankton biomass in South San Francisco Bay? Mar Ecol Prog Ser 9:191–202

Cloern JE (1996) Phytoplankton bloom dynamics in coastal ecosystems: a review with some general lessons from sustained investigation of San Francisco Bay, California. Rev Geophys 34:127–168

Cloern JE, Jassby AD (2008) Complex seasonal patterns of primary producers at the land-sea interface. Ecol Lett 11: 1294–1303

Cloern JE, Jassby AD (2010) Patterns and scales of phytoplankton variability in estuarine-coastal ecosystems. Estuaries Coasts 33:230–241

EPA (2001) Nutrient criteria technical guidance manual: estuarine and coastal marine waters. Office of Water, Environmental Protection Agency, Washington, DC

FBFKFS (2002) Comprehensive Everglades Restoration Plan, Project Management Plan, Florida Bay & Florida Keys Feasibility Study. US Army Corps of Engineers and South Florida Water Management District, West Palm Beach, FL

Fourqurean J, Robblee M (1999) Florida Bay: a history of recent ecological changes. Estuaries 22:345–357

Fourqurean JW, Jones RD, Zieman JC (1993) Processes influencing water column nutrient characteristics and phosphorus limitation of phytoplankton biomass in Florida Bay, FL, USA: inferences from spatial distributions. Estuar Coast Shelf Sci 36:295–314

Gameiro C, Zwolinski J, Brotas V (2011) Light control on phytoplankton production in a shallow and turbid estuarine system. Hydrobiologia 669:249–263

Glibert P, Heil C, Hollander D, Revilla M, Hoare A, Alexander J, Murasko S (2004) Evidence for dissolved organic

nitrogen and phosphorus uptake during a cyanobacterial bloom in Florida Bay. Mar Ecol Prog Ser 280:73–83
Glibert PM, Heil CA, Rudnick DT, Madden CJ, Boyer JN, Kelly SP (2009) Florida Bay: water quality status and trends, historic and emerging algal bloom problems. Contrib Mar Sci 38:5–17
Goleski JA, Koch F, Marcoval M a., Wall CC, Jochem FJ, Peterson BJ, Gobler CJ (2010) The role of zooplankton grazing and nutrient loading in the occurrence of harmful cyanobacterial blooms in Florida Bay, USA. Estuaries Coasts 33:1202–1215
Grömping U (2006) Relative importance for linear regression in R: the package relaimpo. J Stat Softw 17:139–147
Hall MO, Durako MJ, Fourqurean JW, Zieman JC (1999) Decadal changes in seagrass distribution and abundance in Florida Bay. Estuaries 22:445–459
Hansen M, DeWitt NT (2000) 1890 and 1990 bathymetry of Florida Bay. Report 00-347. US Geological Survey, St Petersburg, Florida
Hart JA, Phlips EJ, Badylak S, Dix N and others (2015) Phytoplankton biomass and composition in a well-flushed, sub-tropical estuary: the contrasting effects of hydrology, nutrient loads and allochthonous influences. Mar Environ Res 112:9–20
Heil CA, Revilla M, Glibert PM, Murasko S (2007) Nutrient quality drives differential phytoplankton community composition on the southwest Florida shelf. Limnol Oceanogr 52:1067–1078
Helsel DR, Hirsch RM (2002) Statistical methods in water resources. Techniques of water-resources investigations of the United States Geological Survey. Book 4, Hydrologic Analysis and Interpretation. USGS, Reston, VA
Kelble CR, Ortner PB, Hitchcock GL, Boyer JN (2005) Attenuation of photosynthetically available radiation (PAR) in Florida Bay: potential for light limitation of primary producers. Estuaries 28:560–571
Kelble CR, Johns EM, Nuttle WK, Lee TN, Smith RH, Ortner PB (2007) Salinity patterns of Florida Bay. Estuar Coast Shelf Sci 71:318–334
Koenker RW, Bassett G (1978) Regression quantiles. Econometrica 46:33–50
Lavrentyev PJ, Bootsma HA, Johengen TH, Cavaletto JF, Gardner WS (1998) Microbial plankton response to resource limitation: insights from the community structure and seston stoichiometry in Florida Bay, USA. Mar Ecol Prog Ser 165:45–57
Lawrence D, Dagg MJ, Liu H, Cummings SR, Ortner PB, Kelble C (2004) Wind events and benthic-pelagic coupling in a shallow subtropical bay in Florida. Mar Ecol Prog Ser 266:1–13
Lee TN, Johns E, Melo N, Smith RH, Ortner P, Smith D (2006) On Florida Bay hypersalinity and water exchange. Bull Mar Sci 79:301–327
Lindeman RH, Merenda PF, Gold RZ (1980) Introduction to bivariate and multivariate analysis. Addison-Wesley, Glenview, IL
Lynch TC, Phlips EJ (2000) Filtration of the bloom-forming cyanobacteria *Synechococcus* by three sponge species from Florida Bay, USA. Bull Mar Sci 67:923–936
Madden C, McDonald A (2009) Florida Bay SEACOM: Seagrass Ecological Assessment and Community Organization Model. South Florida Water Management District Coastal Ecosystems Division, West Palm Beach, FL
McIvor CC, Ley JA, Bjork RD (1994) Changes in freshwater inflow from the Everglades to Florida Bay including effects on biota and biotic processes: a review. In: Davis SM, Ogden JC (ed) Everglades: the ecosystem and its restoration. St Lucie Press, Delray Beach, FL, p 117–146
Melesse AM, Krishnaswamy J, Zhang K (2008) Modeling coastal eutrophication at Florida bay using neural networks. J Coast Res 24:190–196
Mitchell JM, Dzerdzeevskii B, Flohn H, Hofmeyr WL, Lamb HH, Rao KN, Wallen CC (1966) Climatic change. Technical Note No. 79. World Meteorological Organization, Geneva
Monsen NE, Cloern JE, Lucas LV, Monismith SG (2002) The use of flushing time, residence time, and age as transport time scales. Limnol Oceanogr 47:1545–1553
Montgomery DC, Peck EA (1992) Introduction to linear regression analysis. Wiley, Hoboken, NJ
Moriasi DN, Arnold JG, Van Liew MW, Binger RL, Harmel RD, Veith TL (2007) Model evaluation guidelines for systematic quantification of accuracy in watershed simulations. Trans ASABE 50:885–900
Nuttle WK, Fourqurean JW, Cosby BJ, Zieman JC, Robblee B (2000) Influence of net freshwater supply on salinity in Florida Bay. Water Resour Res 36:1805–1822
Peterson BJ, Chester CM, Jochem FJ, Fourqurean JW (2006) Potential role of sponge communities in controlling phytoplankton blooms in Florida Bay. Mar Ecol Prog Ser 328:93–103
Phlips EJ, Badylak S (1996) Spatial variability in phytoplankton standing crop and composition in a shallow inner-shelf lagoon, Florida Bay, Florida. Bull Mar Sci 58: 203–216
Phlips EJ, Lynch TC, Badylak S (1995) Chlorophyll *a*, tripton, color, and light availability in a shallow tropical inner-shelf lagoon, Florida Bay, USA. Mar Ecol Prog Ser 127:223–234
Phlips EJ, Badylak S, Lynch TC (1999) Blooms of the picoplanktonic cyanobacterium *Synechococcus* in Florida Bay, a subtropical inner-shelf lagoon. Limnol Oceanogr 44:1166–1175
Phlips EJ, Badylak S, Hart J, Haunert D and others (2012) Climatic influences on autochthonous and allochthonous phytoplankton blooms in a subtropical estuary, St. Lucie Estuary, Florida, USA. Estuaries Coasts 35:335–352
Politis DN, Romano JP (1994) The stationary bootstrap. J Am Stat Assoc 89:1303–1313
R Core Team (2015) R: A language and environment for statistical computing.
Reynolds C (2006) Ecology of phytoplankton. Cambridge University Press, Cambridge
Richardson B (2009) Physiological characteristics and competitive strategies of bloom-forming cyanobacteria and diatoms of Florida Bay. Contrib Mar Sci 38:19–36
Ritter A, Muñoz-Carpena R (2013) Performance evaluation of hydrological models: Statistical significance for reducing subjectivity in goodness-of-fit assessments. J Hydrol 480:33–45
Rudnick DT, Chen Z, Childers DL, Boyer JN, Fontaine TD (1999) Phosphorus and nitrogen inputs to Florida Bay: the importance of the everglades watershed. Estuaries 22:398–416
Rudnick DT, Ortner PB, Browder JA, Davis SM (2005) A conceptual ecological model of Florida Bay. Wetlands 25: 870–883
Santer BD, Wigley TML, Boyle JS, Gaffen DJ and others (2000) Statistical significance of trends and trend differences in layer-average atmospheric temperature time

series. J Geophys Res 105:7337–7356
Santschi P, Höhener P, Benoit G, Buchholtz-ten Brink M (1990) Chemical processes at the sediment–water interface. Mar Chem 30:269–315
Sonderegger DL, Wang H, Clements WH, Noon BR (2009) Using SiZer to detect thresholds in ecological data. Front Ecol Environ 7:190–195
The MathWorks Inc (2015) MATLAB 8.6. Natick, MA. www.mathworks.com
Thompson JK, Koseff JR, Monismith SG, Lucas LV (2008) Shallow water processes govern system-wide phytoplankton bloom dynamics: a field study. J Mar Syst 74: 153–166
Ward BA, Dutkiewicz S, Follows MJ (2014) Modelling spatial and temporal patterns in size-structured marine plankton communities: top-down and bottom-up controls. J Plankton Res 36:31–47
Winder M, Cloern JE (2010) The annual cycles of phytoplankton biomass. Philos Trans R Soc B 365:3215–3226
Xu Y, Schroth AW, Isles PDF, Rizzo DM (2015) Quantile regression improves models of lake eutrophication with implications for ecosystem-specific management. Freshw Biol 60:1841–1853
Zhang JZ, Fischer CJ, Ortner PB (2004) Potential availability of sedimentary phosphorus to sediment resuspension in Florida Bay. Global Biogeochem Cycles 18:1–14
Zhao J, Hu C, Lapointe B, Melo N, Johns EM, Smith RH (2013) Satellite-observed black water events off southwest Florida: implications for coral reef health in the Florida Keys National Marine Sanctuary. Remote Sens 5: 415–431
Zieman JC, Fourqurean JW, Iverson RL (1989) Distribution, abundance and productivity of seagrasses and macroalagae in Florida Bay. Bull Mar Sci 44:292–311
Zuur AF, Ieno EN, Smith GM (2007) Analysing ecological data. Springer Science+Business Media, New York, NY

Editorial responsibility: Steven Lohrenz, New Bedford, Massachusetts, USA

Submitted: May 18, 2016; Accepted: January 11, 2017
Proofs received from author(s): February 27, 2017